

## ORIGINAL ARTICLE

# Effective design of barrier enclosure to contain aerosol emissions from COVID-19 patients

Dan Daniel<sup>1</sup> | Marcus Lin<sup>2</sup> | Irvan Luhung<sup>3</sup> | Tony Lui<sup>4</sup> | Anton Sadovoy<sup>1</sup> | Xueqi Koh<sup>1</sup> | Anqi Sng<sup>1</sup> | Tuan Tran<sup>2</sup> | Stephan C. Schuster<sup>3</sup> | Xian Jun Loh<sup>1</sup> | Oo Schwe Thet<sup>5</sup> | Chee Keat Tan<sup>4</sup>

<sup>1</sup>Institute of Materials Research and Engineering, A\*STAR (Agency for Science, Technology and Research, Innovis, Singapore

<sup>2</sup>School of Mechanical and Aerospace Engineering, Nanyang Technological University, Singapore

<sup>3</sup>Singapore Centre For Environmental Life Sciences Engineering (SCELSE, Nanyang Technological University, Singapore, Singapore

<sup>4</sup>Ng Teng Fong General Hospital, Singapore, Singapore

<sup>5</sup>School of Engineering, Ngee Ann Polytechnic, Singapore, Singapore

## Correspondence

Dan Daniel, Institute of Materials Research and Engineering, A\*STAR (Agency for Science, Technology and Research), 2 Fusionopolis Way, Innovis, Singapore 138634.

Email: daniel@imre.a-star.edu.sg

Oo Schwe Tet, School of Engineering, Ngee Ann Polytechnic, 535 Clementi Road, Singapore 5994.

Email: thet\_oo\_shwe@np.edu.sg

Chee Keat Tan, Ng Teng Fong General Hospital, 1 Jurong East Street 21, Singapore 609606.

Email: chee\_keat\_tan@nuhs.edu.sg

## Funding information

A\*STAR, Grant/Award Number: SC25/20-8R1640; National Medical Research Council, Singapore, Grant/Award Number: MOH-000411

## Abstract

Facing shortages of personal protective equipment, some clinicians have advocated the use of barrier enclosures (typically mounted over the head, with and without suction) to contain aerosol emissions from coronavirus disease 2019 (COVID-19) patients. There is, however, little evidence for its usefulness. To test the effectiveness of such a device, we built a manikin that can expire micron-sized aerosols at flow rates close to physiological conditions. We then placed the manikin inside the enclosure and used a laser sheet to visualize the aerosol leaking out. We show that with sufficient suction, it is possible to effectively contain aerosol from the manikin, reducing aerosol exposure outside the enclosure by 99%. In contrast, a passive barrier without suction only reduces aerosol exposure by 60%.

## KEYWORDS

barrier enclosure, airborne transmissions, COVID-19, aerosol, infection control

## Practical implications

- Barrier enclosure with active suction can be used to minimize aerosol spread from COVID-19 patients.
- Barrier can be made from cheap material such as acrylic and suction can be provided by wall units commonly found in hospitals, that is, this approach can potentially be scaled up.
- Given the growing evidence that COVID-19 is airborne, a well-designed barrier enclosure can provide additional protection for healthcare workers.

## 1 | INTRODUCTION

The prolonged nature of the coronavirus disease 2019 (COVID-19) pandemic has resulted in global shortages of personal protective equipment (PPE), especially N95 respirators. As a result, some clinicians have resorted to using barrier enclosures typically mounted on the hospital bed over the patient's head to contain any aerosol emissions, especially during aerosol generating procedures such as intubation.<sup>1–3</sup> Different barrier designs with varying levels of complexities have been proposed, ranging from a simple carton box,<sup>4</sup> plastic drapes and boxes<sup>1,5,6</sup> to a custom-built acrylic box with active suction and filtration system.<sup>7</sup> Despite all these innovations, there is little validation on the effectiveness of the various designs.

To assess the performance of barrier enclosures, some groups have resorted to simulating a cough/sneeze (for example by using an exploding balloon<sup>1</sup> or a water spray<sup>7</sup>) and comparing the splatter pattern of droplets with and without the enclosure. Such an approach can confirm the effectiveness of the enclosures at blocking larger respiratory droplets (tens of microns to millimeters in diameters), but not for small micron-sized aerosol droplets which are airborne and can potentially travel over much longer distances.<sup>8</sup>

To detect aerosol spread, some groups have successfully used particle counters to measure the concentration of micron and sub-micron droplets leaking out of the barrier enclosure<sup>5,9</sup> and concluded that active suction is critical to effectively contain aerosol droplets.<sup>10</sup> However, the amount of suction required to achieve containment remains unexplored. This is crucial because COVID-19 patients are often subjected to treatment modalities involving high gas flow rates, for example, high flow nasal cannula (HFNC) therapy to provide supplemental oxygen,<sup>11–13</sup> which can quickly disperse bio-aerosol over large distances, increasing the infection risk to healthcare workers.

In this paper, we would like to establish the design criteria—in particular, the minimum suction required—for a barrier enclosure to effectively contain aerosol emissions especially with high (and medically relevant) gas flow rates. We used two complementary techniques (one qualitative and the other quantitative) to assess the performance of the barrier enclosure. The first is to use laser sheets to visualize the aerosol flow from a custom-built manikin

expiring micron-sized water-glycerin droplets at flow rates close to physiological conditions. The second is to collect the aerosol leaking out using air samplers and subsequently to quantify the collected amount using spectrofluorometry.

Given the growing evidence that COVID-19 is airborne and can spread through aerosol,<sup>14–16</sup> a well-designed barrier enclosure can be useful as an additional layer of protection for healthcare workers.

## 2 | MATERIALS AND METHODS

### 2.1 | Barrier enclosure design

The barrier enclosure was designed by local institutions of higher learning and used by a hospital in Singapore. The physical enclosure (width, breadth, and height of 92 cm × 60 cm × 70 cm) is made of acrylic (Figure 1A), with a plastic drape at the front, four openings (two at the headend and one on either side) for access to patients, and two suction ports (one on either side). Suction is provided by two wall units (BeaconMedaes Gem 10) typically found in a hospital, each with a maximum suction rate of  $Q_{\text{suction}} = 60 \text{ L min}^{-1}$ .

COVID-19 patients typically require supplemental oxygen therapy, with high flow nasal cannula (HFNC) oxygen therapy (Figure 1B,C) showing positive medical outcomes.<sup>11–13</sup> HFNC is a heated and humidified system (typically 100% humidity at 34–37°C) that delivers oxygen passively at a prescribed concentration (between 21% and 100%) at high flow rates up to  $Q_{\text{O}_2} = 60 \text{ L min}^{-1}$ .

In this study, we looked at the effectiveness of aerosol containment for different  $Q_{\text{O}_2} = 0–60 \text{ L min}^{-1}$  (with oxygen concentration set at 75%) and  $Q_{\text{suction}} = 0–120 \text{ L min}^{-1}$ . The HFNC was placed over the nose of a custom-built manikin which can emit aerosol at flow rates close to physiological conditions as described in the next section.

### 2.2 | Manikin design and aerosol generation

Figure 2A shows a schematic of the custom-built manikin. A 400 W fog machine, typically used in entertainment venues, was used to heat up and generate micron-sized aerosol from a glycerin-water



**FIGURE 1** A, Barrier enclosure design used to contain aerosols from (B) patients who typically require supplementary oxygen treatment (C) delivered through a nasal cannula

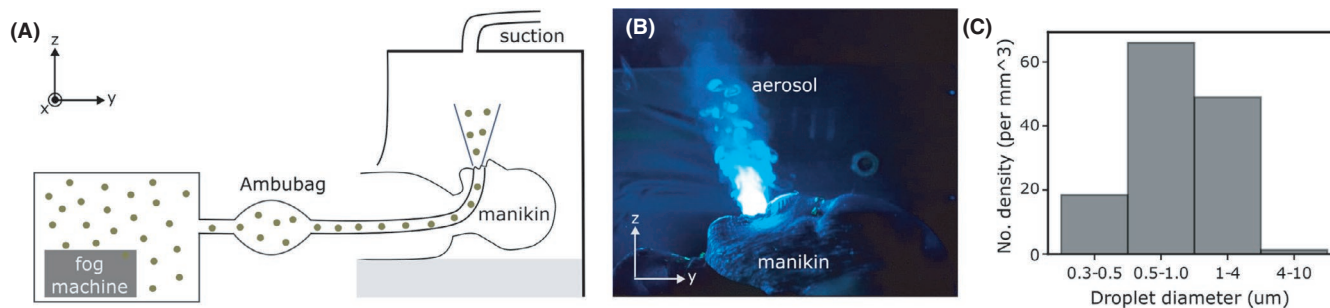


**FIGURE 2** A, Schematic of the custom-built manikin placed inside the barrier enclosure. B, Micron-sized glycerin-water aerosol droplets expelled from the manikin and visualized by shining a blue laser sheet at the sagittal plane (See also Video S1). C, Size distribution of aerosol droplets

mixture (50 v%) inside a 50 cm × 50 cm × 60 cm box within 3 seconds. Food-grade glycerin was purchased from a baking shop. The addition of glycerin which has a boiling point of 290°C minimizes the evaporation of the aerosol droplets.

A manual resuscitator or an Ambu bag was then used to transfer the aerosol from the box through the mouth of the manikin into the barrier. The Ambu bag was compressed by hand and the volume pushed out during each compression cycle ( $0.63 \pm 0.03$  L) was determined by releasing the expelled air into a jar filled with water and measuring the volume of water displaced. The length of the compression cycle (3 s) was chosen to closely mimic the physiological parameters of the human breath, that is,  $Q_{\text{air}} = 13 \text{ L min}^{-1}$ . We did not find significant difference in the expelled volumes between different human operators.

In a typical experiment, the Ambu bag was compressed for 3 seconds and re-inflated for another 3 seconds to mimic continuous exhalation of aerosol for 20 minutes (Figure 2B and Video S1). A metronome was used to help the operator keep in time. The manikin does not simulate the inhalation cycle, but this should not affect the results greatly, since aerosol is generated mostly during the exhalation cycle.

Aerosol typically refers to droplets  $< 5 \mu\text{m}$  in diameter and thought to be responsible for airborne transmission of diseases, since they can stay suspended in air for a long period of time.<sup>17,18</sup> Aerosol generated during respiratory activities (such as talking and coughing) and in healthcare settings (such as intubation) is thought to vary between 0.1 and 10  $\mu\text{m}$ .<sup>18-20</sup> The droplets generated by the fog machine span this range with a mean diameter of about 1  $\mu\text{m}$ , as measured using a particulate matter sensor Sensirion SPS30 (Figure 2C).

### 2.3 | Visualizing aerosol flow using laser sheets

The aerosol flow can be visualized by shining 2D laser sheets. The laser sheet is generated by passing a laser light (Class 3B, 100 mW power) through a 4-mm-diameter cylindrical rod lens (Edmund Optics). Similar techniques have been used to visualize aerosol leak from masks and faceshields.<sup>21</sup>

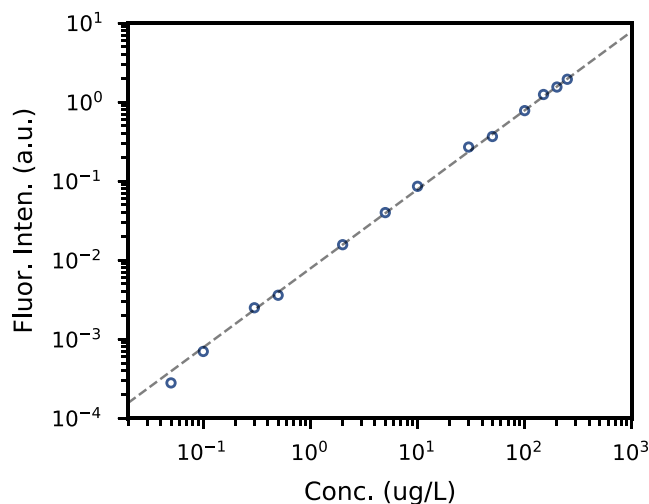


**FIGURE 3** Calibration curve for different concentration standards. Dashed line is the best fit curve with a slope of 1, that is, intensity is linearly proportional to concentration

### 2.4 | Quantifying aerosol leak

We first dissolved a small amount of fluorescein sodium salt (Sigma Aldrich) at a concentration of 0.5 g L<sup>-1</sup> in the water-glycerin solution. The aerosol (glycerol-water droplets with fluorescein) leaking out of the barrier enclosure was collected using SASS 3100 Air Samplers fitted with standard filter cartridges from Research International running at a flow rate of 60 L min<sup>-1</sup> for 20 minutes. The hospital room we were using had a total air change rate per hour of 10, that is, it took about 6 minutes for the air in the room to be well-mixed, shorter than the experimental time.

SASS 3100 air sampler has been used previously to collect bio-aerosols from the air.<sup>22</sup> The filter paper was then placed in a tube of 2 mL of deionized (DI) water and shaken with a vortex mixer for 1 minute to dissolve the trapped fluorescein. Fluorescein has an excitation and emission wavelengths of 490 and 514 nm, respectively. The fluorescein concentration (and hence the amount of fluorescein) in the 2 mL solution was then determined using a spectrofluorometer

(Duetta, HORIBA scientific) by comparing its fluorescence intensity at 514 nm with those from calibration standards of known concentrations (See Figure 3 for the calibration curve). The minimum concentration that can be measured using spectrofluorometer is  $0.02 \mu\text{g L}^{-1}$  or  $0.04 \text{ ng}$  in  $2 \text{ mL}$  solution.

### 3 | RESULTS AND DISCUSSIONS

#### 3.1 | Minimum suction required for effective containment of aerosol

For aerosol to be effectively contained, we need to generate a negative pressure inside the enclosure. This is achieved when the flow rate of the suction  $Q_{\text{suction}}$  exceeds the sum of the oxygen flow rate  $Q_{\text{O}_2}$  and the expiration rate of the patient/manikin  $Q_{\text{air}}$ , that is,

$$Q_{\text{suction}} > Q_{\text{O}_2} + Q_{\text{air}} \quad (1)$$

For example, at the maximum oxygen flow rate  $Q_{\text{O}_2} = 60 \text{ L min}^{-1}$ , we are able to contain aerosol emissions by turning on the two suction wall units with a combined  $Q_{\text{suction}} = 120 \text{ L min}^{-1}$  (Figure 4A and Video S2). To visualize the aerosol flow, we shone two laser sheets: a blue laser sheet at the sagittal z-y plane and a green laser sheet at the transverse x-z plane in front of the barrier. As expected, there

is no aerosol leakage and the green laser sheet is not visible since there is minimal aerosol outside the barrier to scatter the light. We also observed fresh air, which was free from aerosol and therefore appeared dark, continually being drawn through gaps at the bottom of the plastic drape.

In contrast, with just one ( $Q_{\text{suction}} = 60 \text{ L min}^{-1}$ ) or no suction ( $Q_{\text{suction}} = 0 \text{ L min}^{-1}$ ), the aerosol cannot be contained and spread quickly throughout the entire room (with a floor area of about  $30 \text{ m}^2$ ) within minutes. The aerosol leaking out scatters light strongly and renders the green laser sheet visible (Figure 4B and Video S3).<sup>23</sup> The enclosure chamber is also now completely filled with aerosol, and there is no fresh air being drawn in.

To test the effectiveness of the aerosol containment under different conditions, we varied the suction rate  $Q_{\text{suction}}$  from 0 (no suction) to 60 and  $120 \text{ L min}^{-1}$  (1 and 2 wall suction units, respectively), while at the same time subjecting the manikin to different oxygen flow rates  $Q_{\text{O}_2} = 0, 30$  and  $60 \text{ L min}^{-1}$  (Figure 4C). Experimentally, we found that Equation 1 correctly predicts the criterion for effective aerosol confinement (The transition from effective to ineffective containment as predicted by Equation 1 is indicated by the gray line in Figure 4C).

In our experiment, the suction ports are located on the two sides of the enclosure. The exact positionings of the suction port, together with the detailed geometry of the enclosure, need to be optimized to avoid deadspots, where there are little circulation and potential



FIGURE 4 A, Aerosol is effectively contained when  $Q_{\text{suction}} > Q_{\text{O}_2} + Q_{\text{air}}$ . B, Otherwise, aerosol leakage from the enclosure can be readily observed. C, Phase diagram for effective (blue filled dots) and ineffective aerosol containment (unfilled red dots)

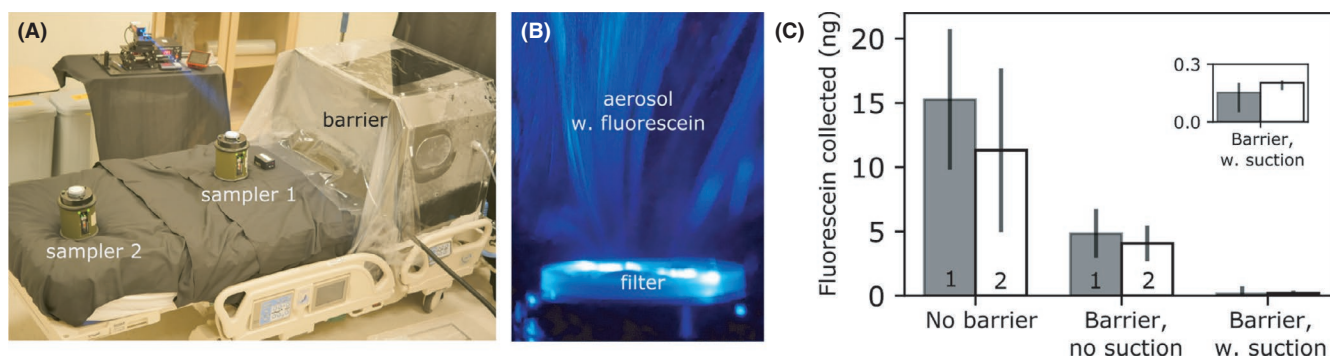


FIGURE 5 A, To collect the aerosol leaking out, we placed two air samplers outside the barrier enclosure. B, Aerosol droplets (with added fluorescein) were trapped by the filter on the air sampler, which can then be detected using spectrofluorometer. C, The amount of fluorescein collected by air samplers 1 and 2 for enclosure barrier with and without suction can then be compared to the control, that is, no barrier. Error bars are the standard deviation for triplicates

accumulation of aerosol. This can be done using detailed computational fluid dynamics study and could be part of a future study.

### 3.2 | Reduction in aerosol exposure

To assess the level of protection afforded by the barrier enclosure with and without suction, we added a small amount of fluorescein to the water-glycerin solution. The level of aerosol exposure can then be quantified by measuring the amount of fluorescein collected by filters of two air samplers placed 50 and 110 cm away from the barrier (samplers 1 and 2 in Figure 5A, respectively). The amount of fluorescein trapped by the filter (Figure 5B) can be deduced by spectrofluorometry. See Section 1D, for experimental details.

We found that for HFNC oxygen therapy with no barrier at  $Q_{O_2} = 60 \text{ L min}^{-1}$ , the amount of fluorescein collected after 20 minutes by samplers 1 and 2 are  $15 \pm 5 \text{ ng}$  and  $11 \pm 6 \text{ ng}$ , respectively (Figure 5C). With a passive barrier and no suction (corresponding to Figure 4B and case *b* in Figure 4C), the amount of fluorescein collected by samplers 1 and 2 was reduced by about 60% to  $5 \pm 2$  and  $4 \pm 1 \text{ ng}$ , respectively. At maximum suction of  $Q_{\text{suction}} = 120 \text{ L min}^{-1}$  (corresponding to Figure 4A and case *a* in Figure 4C), the amount of fluorescein reaching the two samplers was reduced by 99% to  $0.15 \pm 0.08$  and  $0.19 \pm 0.01 \text{ ng}$ , respectively. The amount of fluorescein collected by the two air samplers is similar to each other, because the aerosol droplets are uniformly distributed within the experimental time of 20 minutes.

Finally, we would like to point out that although a passive barrier with no suction provides some level of protection, large amount of aerosol can accumulate inside the barrier over time, which will be released into the room if the barrier were to be dismantled, for example during a medical emergency.

## 4 | CONCLUSIONS

In short, we have established the criterion for effective containment of aerosol for barrier enclosure, namely that the suction rate must exceed the oxygen flow rate and the expiration rate of the human breath. We show explicitly that for high (and medically relevant) oxygen flowrate of  $60 \text{ L min}^{-1}$ , it is possible to significantly reduce aerosol exposure outside the enclosure by 99% with sufficient suction. Given that the barrier enclosure can be made from readily available material such as acrylic and that suction points are commonly found in hospital rooms, we believe such a device can potentially be scaled up and provide additional protection for healthcare workers.

### ACKNOWLEDGEMENTS

The authors would like to acknowledge funding from A\*STAR, Singapore, "A\*CRUSE project on airflow and aerosol particles studies for public agencies" project number SC25/20-8R1640, as well

as from the National Medical Research Council, Singapore, project number MOH-000411.

### CONFLICT OF INTERESTS

Ngee Ann Polytechnic and Ng Teng Fong general Hospital have filed a patent submission for the barrier enclosure design.

### AUTHORS' CONTRIBUTIONS

D.D., L.X.J., C.K.T., and O.S.T. conceived the research idea and supervised the research. O.S.T. and C.K.T. designed and built the barrier enclosure. D.D., M.L., T.L., A.S., X.K., and T.T. contributed to the laser visualization experiment. I.L., S.S., and A.S. performed the air sampling and subsequent fluorescein quantification. D.D. and C.K.T. wrote up the manuscript. All authors have read and approved the manuscript.

### PEER REVIEW

The peer review history for this article is available at <https://publons.com/publon/10.1111/ina.12828>.

### DATA AVAILABILITY STATEMENT

The data that support the findings of this study are available from the corresponding author upon reasonable request.

### REFERENCES

- Canelli R, Connor CW, Gonzalez M, Nozari A, Ortega R. Barrier enclosure during endotracheal intubation. *N Engl J Med*. 2020;382:1957-1958.
- Kovatsis PG, Matava CT, Peyton JM. More on barrier enclosure during endotracheal intubation. *N Engl J Med*. 2020;382:e69.
- Motara F, Laher AE, du Plessis J, Moolla M. The intubox: enhancing frontline healthcare worker safety during Coronavirus disease 2019 (COVID-19). *Cureus*. 2020;12:e8530.
- Lai YY, Chang CM. A carton-made protective shield for suspicious/confirmed COVID-19 intubation and extubation during surgery. *Anesth Analg*. 2020;131(1):e31-e33.
- Simpson JP, Wong DN, Verco L, Carter R, Dzidowski M, Chan PY. Measurement of airborne particle exposure during simulated tracheal intubation using various proposed aerosol containment devices during the COVID-19 pandemic. *Anaesthesia*. 2020;75:1587-1595.
- Kinjo S, Dudley M, Sakai N. Modified wake forest type protective shield for an asymptomatic, COVID-19 nonconfirmed patient for intubation undergoing urgent surgery. *Anesth Analg*. 2020;131:e127-e128.
- Teichert-Filho R, Baldasso CN, Campos MM, Gomes MS. Protective device to reduce aerosol dispersion in dental clinics during the COVID-19 pandemic. *Int Endod J*. 2020;53:1588-1597.
- Bourouiba L, Dehandschoewercker E, Bush JWM. Violent expiratory events: on coughing and sneezing. *J Fluid Mech*. 2014;745:537-563.
- Lang L, Shaw KM, Lozano R, Wang J. Effectiveness of a negative-pressure patient isolation hood shown using particle count. *Br J Anaesth*. 2020;125:e295-e296.
- United States Food and Drug Administration. Protective Barrier Enclosures Without Negative Pressure Used During the COVID-19 Pandemic May Increase Risk to Patients and Health Care Providers - Letter to Health Care Providers. <https://www.fda.gov/medicaldevices/letters-health-care-providers/protective-barrierenclosure>

- es-without-negative-pressure-used-during-covid-19-pandemic-may-increase 2020. accessed: 2020-11-05.
11. Rochweg B, Granton D, Wang DX, et al. High flow nasal cannula compared with conventional oxygen therapy for acute hypoxemic respiratory failure: a systematic review and meta-analysis. *Intensive Care Med.* 2019;45:563-572.
  12. Li J, Fink JB, Ehrmann S. High-flow nasal cannula for COVID-19 patients: low risk of bio-aerosol dispersion. *Eur Respir J.* 2020;55:2000892.
  13. Calligaro GL, Lalla U, Audley G, et al. The utility of high-flow nasal oxygen for severe COVID-19 pneumonia in a resourceconstrained setting: A multi-centre prospective observational study. *EClinicalMedicine.* 2020;28:100570.
  14. Morawska L, Milton DK. It is time to address airborne transmission of COVID-19. *Clin Infect Dis.* 2020;71:2311-2313. <https://doi.org/10.1093/cid/ciaa939>
  15. van Doremalen N, Bushmaker T, Morris DH, et al. Aerosol and surface stability of SARS-CoV-2 as compared with SARS-CoV-1. *N Eng J Med.* 2020;382:1564-1567.
  16. Somsen GA, van Rijn C, Kooij S, Bem RA, Bonn D. Small droplet aerosols in poorly ventilated spaces and SARS-CoV-2 transmission. *Lancet Respir Med.* 2020;8:658-659.
  17. Natural ventilation for infection control in health-care settings, Chap. Annex C.
  18. Morawska LJGR, Johnson GR, Ristovski ZD, et al. Size distribution and sites of origin of droplets expelled from the human respiratory tract during expiratory activities. *J Aerosol Sci.* 2009;40:256-269.
  19. Wilson N, Corbett S, Tovey E. Airborne transmission of covid-19. *Br Med J.* 2020;370:m3206.
  20. Tran K, Cimon K, Severn M, Pessoa-Silva CL, Conly J. Aerosol generating procedures and risk of transmission of acute respiratory infections to healthcare workers: a systematic review. *PLoS One.* 2012;7:e35797.
  21. Verma S, Dhanak M, Frankenfield J. Visualizing droplet dispersal for face shields and masks with exhalation valves. *Phys Fluids.* 2020;32:091701.
  22. Gusareva ES, Acerbi E, Lau KJX, et al. Microbial communities in the tropical air ecosystem follow a precise diel cycle. *Proc Natl Acad Sci USA.* 2019;116:23299-23308.
  23. Gouesbet G, Gréhan G. Generalized lorenz-mie theories. 31 (Springer, 2011). <https://link.springer.com/book/10.1007/978-3-642-17194-9>

## SUPPORTING INFORMATION

Additional supporting information may be found online in the Supporting Information section.

**How to cite this article:** Daniel D, Lin M, Luhung I, et al. Effective design of barrier enclosure to contain aerosol emissions from COVID-19 patients. *Indoor Air.* 2021;31:1639-1644. <https://doi.org/10.1111/ina.12828>